

Journal of Mechanics of Materials and Structures

**CONTOURS FOR PLANAR CRACKS GROWING IN THREE DIMENSIONS:
ILLUSTRATION FOR TRANSVERSELY ISOTROPIC SOLID**

Louis Milton Brock

Volume 10, No. 4

July 2015



CONTOURS FOR PLANAR CRACKS GROWING IN THREE DIMENSIONS: ILLUSTRATION FOR TRANSVERSELY ISOTROPIC SOLID

LOUIS MILTON BROCK

Three-dimensional dynamic steady state growth of a semi-infinite plane crack in a transversely isotropic solid is considered. Growth takes place on a principal plane with the material symmetry axis as one tangent. Fracture is brittle, and driven by compressive loads that translate on the crack surfaces. Translation speed is constant and subcritical, but direction with respect to the principal axes is arbitrary. An analytical solution is obtained, and examined in light of the dynamic energy release rate criterion for the case of a translating compressive point force. Introduction of quasispherical coordinates leads to a nonlinear first-order differential equation for the distance between force and crack edge. The equation depicts a crack edge that tends to the rectilinear away from the force. An analytical expression for the distance measured parallel to translation direction indicates a marked deviation from the rectilinear near the point force.

Introduction

A major goal of fracture mechanics is the determination of crack edge location. In 2D dynamic fracture, this requires an equation of motion for the crack tip [Freund 1990]. In a 3D study, such an equation must describe the crack contour. This goal has been achieved for semi-infinite crack growth in an unbounded isotropic solid [Brock 2015]. This paper extends the analysis to an unbounded transversely isotropic solid. For simplicity, the crack remains in its original plane, which is a principal plane. Moreover, crack growth is caused by compression loads on the crack surface that translate at constant subcritical speed in a fixed direction, and achieves a dynamic steady state.

Two-dimensional dynamic analyses of transversely isotropic half-spaces in which the material symmetry axis coincides with the surface normal essentially correspond to those for the isotropic case, e.g., [Scott and Miklowitz 1967]. As seen in sliding contact analysis [Brock 2013], elastic properties associated with principal planes other than that on the surface do influence 3D results but the solution forms resemble those for the isotropic case. When the surface normal is not the material symmetry axis, however, 3D solution forms are quite distinctive. Therefore, to enhance the effect of anisotropy, (a) the principal plane in this 3D illustration includes the axis of material symmetry, and (b) the fixed direction is arbitrary with respect to this axis.

Two-dimensional analyses of fracture for the general anisotropic solid in the dynamic steady state exist, of course. Indeed, the semi-infinite interface crack has been examined by Willis [1971]. Principal axes define both in-plane coordinates and interface, and the crack edge exhibits the well-known oscillatory behavior. Nevertheless, as in [Brock 2015] and the present study, a formula for crack extension based on dynamic energy release rate is developed.

Keywords: 3D, dynamic, criteria, analytic solution, crack contour, transverse isotropy, energy release.

Analysis begins by considering the unmixed boundary value problem for a discontinuity in displacement imposed over a semi-infinite plane area A_C contained in an unbounded solid. This is of course a dislocation problem and is a standard [Willis 1971; Barber 1992] first step in fracture analysis. For efficiency in application to the title problem, this study considers a discontinuity that vanishes along area boundary B_C , vanishes at infinite distances from it, and translates with A_C at constant subcritical speed V in a fixed direction. A dynamic steady state ensues and allows use of a translating Cartesian basis. The transform solution is generated, but a quasipolar coordinate system is introduced in the inversion process. Expressions for normal traction on the plane of A_C lead to a classical singular integral equation for the displacement discontinuity produced were A_C a crack subject to a prescribed surface load. Imposition of a fracture criterion leads to a nonlinear first-order differential equation for the distance from a given point in A_C to any point on (now) crack edge B_C .

Displacement discontinuity growth — governing equations

Consider an unbounded, transversely isotropic and linearly elastic solid. Cartesian basis $\mathbf{x} = \mathbf{x}(x_k)$ defines the principal material axes. The semi-infinite planar region A_C ($x_3 = 0, x_V < 0$) with rectilinear boundary B_C ($x_V = 0$) is subject to discontinuity

$$[\mathbf{u}(u_k)] = \mathbf{U}(U_k). \tag{1}$$

Here $k = (1, 2, 3)$, $[]$ signifies a jump as travel from $x_3 = 0-$ to $x_3 = 0+$ occurs, \mathbf{u} is the displacement field and discontinuity components $U_k = U_k(x_1, x_2)$. The x_2 -direction defines the axis of material symmetry, and

$$x_V = x_1 \cos \theta + x_2 \sin \theta, \quad |\theta| < \frac{\pi}{2}. \tag{2a}$$

The region translates in the positive x_V -direction at constant subcritical speed V . A dynamic steady state is achieved by (\mathbf{U}, A_C) , and boundary B_C may no longer be rectilinear. Displacement $\mathbf{u}(u_k)$ and traction $\mathbf{T}(\sigma_{ik})$ do not vary in the moving frame of A_C . Basis \mathbf{x} is therefore translated with A_C so that $u_k = u_k(\mathbf{x})$, $U_k = U_k(x_1, x_2)$, $\sigma_{ik} = \sigma_{ik}(\mathbf{x})$, and the time derivative can be written

$$-V \partial_V, \quad \partial_V = \partial_1 \cos \theta + \partial_2 \sin \theta. \tag{2b}$$

Here ∂_k signifies x_k -differentiation. For convenience, $\mathbf{x} = 0$ is located in the region of discontinuity, so that function $\mathfrak{S}(x_1, x_2) = 0, \sqrt{x_1^2 + x_2^2} \neq 0$ defines contour B_C and the region can be defined as $(x_1, x_2) \in A_C$. Both \mathfrak{S} and its gradient $\nabla \mathfrak{S}$ are continuous, and any line passing through $\mathbf{x} = 0$ in the $x_1 x_2$ -plane can cross B_C only once. For $x_3 \neq 0$, governing equations for $\mathbf{u}(x_k)$ can be written as [Brock 2013]

$$\nabla \cdot \mathbf{T} = C_{44} V^2 \partial_V^2 \mathbf{u}, \tag{3a}$$

$$\begin{bmatrix} \sigma_{11} \\ \sigma_{22} \\ \sigma_{33} \end{bmatrix} = \begin{bmatrix} C_{11} & C_{12} & C_{13} \\ C_{12} & C_{22} & C_{12} \\ C_{13} & C_{12} & C_{11} \end{bmatrix} \begin{bmatrix} \partial_1 u_1 \\ \partial_2 u_2 \\ \partial_3 u_3 \end{bmatrix}, \tag{3b}$$

$$\sigma_{2k} = C_{44} (\partial_2 u_k + \partial_k u_2) \quad \text{for } k = 1, 3, \quad \text{and } \sigma_{31} = C_{55} (\partial_3 u_1 + \partial_1 u_3). \tag{3c}$$

Here $(C_{11}, C_{22}, C_{12}, C_{13}, C_{44}, C_{55})$ are the elastic constants, and $C_{13} = C_{11} - 2C_{55}$ [Jones 1999]. As reference quantities, we adopt shear modulus and shear wave speed

$$\mu = C_{44}, \quad V_S = \sqrt{C_{44}/\rho}. \quad (4a)$$

Here ρ is mass density, and (4a) gives the dimensionless terms

$$c = \frac{V}{V_S}, \quad d_1 = \frac{C_{11}}{C_{44}}, \quad d_2 = \frac{C_{22}}{C_{44}}, \quad d_5 = \frac{C_{55}}{C_{44}}, \quad d_{12} = \frac{C_{12}}{C_{44}}, \quad d_{13} = \frac{C_{13}}{C_{44}} = d_1 - 2d_5. \quad (4b)$$

In light of (1), conditions for $x_3 = 0$ are

$$[u_k] = U_k \quad \text{for } (x_1, x_2) \in A_C, \quad [u_k] = 0 \quad \text{for } (x_1, x_2) \notin A_C, \quad (5a)$$

$$[\sigma_{3k}] = 0. \quad (5b)$$

Components U_k are not specified, but must be finite and continuous for $(x_1, x_2) \in A_C$. Therefore $U_k = 0$ for $\Im(x_1, x_2) = 0$, and (\mathbf{u}, \mathbf{T}) should remain finite for $|\mathbf{x}| \rightarrow \infty, x_3 \neq 0$.

General transform solution

A double bilateral transform [Sneddon 1972] can be defined as

$$\hat{F} = \iint F(x_1, x_2) \exp(-p_1 x_1 - p_2 x_2) dx_1 dx_2. \quad (6)$$

Integration is along the entire $\text{Re}(x_1)$ - and $\text{Re}(x_2)$ -axes. Application of (6) to (3) gives

$$\hat{\mathbf{u}} = \hat{\mathbf{u}}_5 + \hat{\mathbf{u}}_+ + \hat{\mathbf{u}}_-, \quad (7a)$$

$$\hat{\mathbf{u}}_5 = U_5^{(\pm)} \exp(-B_5 |x_3|), \quad \hat{\mathbf{u}}_{\pm} = U_{\pm}^{(\pm)} \exp(-A_{\pm} |x_3|). \quad (7b)$$

In (7b) superscript (\pm) signifies $x_3 \geq 0$ and $x_3 \leq 0$, respectively, and

$$(U_5)_1^{(\pm)} = (\pm)B_5 V_5^{(\pm)}, \quad (U_5)_2^{\pm} = 0, \quad (U_5)_3^{(\pm)} = p_1 V_5^{(\pm)}, \quad (8a)$$

$$(U_{\pm})_1^{(\pm)} = -(1 + d_{12})p_1 p_2 V_{\pm}^{(\pm)}, \quad (U_2)_2^{(\pm)} = d_1(A_{\pm}^2 + \Gamma_1)V_{\pm}^{(\pm)}, \quad (8b)$$

$$(U_{\pm})_3^{(\pm)} = (\pm)(1 + d_{12})p_2 A_{\pm} V_{\pm}^{(\pm)}. \quad (8c)$$

Here $(V_5^{(\pm)}, V_{\pm}^{(\pm)})$ are arbitrary functions of (p_1, p_2) and

$$B_5 = \sqrt{-p_1^2 - \Gamma_0/d_5}, \quad T_5 = d_5(p_1^2 - B_5^2), \quad (9a)$$

$$\Gamma_0 = p_2^2 - c^2 p_V^2, \quad p_V = p_1 \cos \theta + p_2 \sin \theta, \quad (9b)$$

$$A_{\pm} = \sqrt{-p_1^2 - \Gamma_{\pm}/d_1}, \quad \Gamma_{\pm} = \frac{1}{2}(M \pm \sqrt{M^2 - 4d_1 \Gamma_2 \Gamma_0}), \quad (9c)$$

$$M = d_1 \Gamma_2 + \Gamma_0 - (1 + d_{12})^2 p_2^2, \quad \Gamma_1 = p_1^2 + \Gamma_0/d_1, \quad \Gamma_2 = d_2 p_2^2 - c^2 p_V^2. \quad (9d)$$

For bounded behavior as $|x_3| \rightarrow \infty$, (7b) requires that $\text{Re}(B_5, A_{\pm}) \geq 0$ in the cut complex (p_1, p_2) -planes. Application of (6) to (3b), (3c) and (5) and substitution of (8) and (9) gives equations for $(V_5^{(\pm)}, V_+^{(\pm)}, V_-^{(\pm)})$ in terms of transforms \hat{U}_k . The solutions are then used to generate expression (A.1)

for $(\hat{\sigma}_{33}, \hat{\sigma}_{31}, \hat{\sigma}_{32})$ in plane $x_3 = 0$. That the x_3 -direction does not correspond to the material symmetry axis is clear from the different forms for (A.1b) and (A.1c).

Transform inversion — general formulas

In (5), inhomogeneous terms (U_1, U_2, U_3) arise only for $(x_1, x_2) \in A_C$. In light of (A.1), therefore, the inversion operation corresponding to (6) gives $(\sigma_{33}, \sigma_{31}, \sigma_{32})$ for $x_3 = 0$ as linear combinations of expressions

$$\iint U_k d\xi_1 d\xi_2 \frac{1}{2\pi i} \int dp_1 \frac{1}{2\pi i} \int P_k dp_2 \exp[p_1(x_1 - \xi_1) + p_2(x_2 - \xi_2)]. \tag{10}$$

Here $U_k = U_k(\xi_1, \xi_2)$ and $P_k = P_k(p_1, p_2)$ is the corresponding coefficient. Double integration is over A_C , and single integration is over the entire $\text{Im}(p_1)$ - and $\text{Im}(p_2)$ -axes. After [Brock 2013; 2015], transformations are introduced:

$$p_1 = p \cos \psi, \quad p_2 = p \sin \psi, \tag{11a}$$

$$\begin{bmatrix} x \\ y \end{bmatrix} = \begin{bmatrix} \cos \psi & \sin \psi \\ -\sin \psi & \cos \psi \end{bmatrix} \begin{bmatrix} x_1 \\ x_2 \end{bmatrix}, \quad \begin{bmatrix} \xi \\ \eta \end{bmatrix} = \begin{bmatrix} \cos \psi & \sin \psi \\ -\sin \psi & \cos \psi \end{bmatrix} \begin{bmatrix} \xi_1 \\ \xi_2 \end{bmatrix}. \tag{11b}$$

In (11a) and (11b), $\text{Re}(p) = 0+$, $|\text{Im}(p), x, y, \xi, \eta| < \infty$ and $|\psi - \theta| < \frac{\pi}{2}$. Parameters $(p, \psi), (x, \psi; y = 0)$ and $(\xi, \psi; \eta = 0)$ resemble quasipolar coordinate systems, i.e.,

$$d\xi_1 d\xi_2 = |\xi| d\xi d\psi, \quad dp_1 dp_2 = |p| dp d\psi. \tag{11c}$$

Use of (11) in (9) give

$$\Gamma_0 = p^2 C_0, \quad \Gamma_1 = p^2 C_1, \quad \Gamma_2 = p^2 C_2, \quad T_5 = p^2 T_5, \tag{12a}$$

$$\Gamma_{\pm} = p^2 C_{\pm}, \quad M = p^2 M, \tag{12b}$$

$$A_{\pm} = A_{\pm} \sqrt{p} \sqrt{-p}, \quad B_5 = B_5 \sqrt{p} \sqrt{-p}. \tag{12c}$$

Equation (12) is based on parameters that depend on (c, ψ, θ) :

$$C_0 = \sin^2 \psi - c_V^2, \quad C_1 = \cos^2 \psi + C_0/d_1, \quad C_2 = d_2 \sin^2 \psi - c_V^2, \tag{13a}$$

$$T_5 = 2d_5 \cos^2 \psi + C_0, \quad c_V = c \cos(\psi - \theta), \tag{13b}$$

$$M = d_1 C_2 + C_0 - (1 + d_{12})^2 \sin^2 \psi, \quad C_{\pm} = \frac{1}{2} (M \pm \sqrt{M^2 - 4d_1 C_2 C_0}), \tag{13c}$$

$$B_5 = \sqrt{\cos^2 \psi + C_0/d_5}, \quad A_{\pm} = \sqrt{\cos^2 \psi + C_{\pm}/d_1}. \tag{13d}$$

If $\text{Re}(B_5, A_{\pm}) \geq 0$, terms in (7) are bounded when branches $\text{Im}(p) = 0, \text{Re}(p) < 0$ and $\text{Im}(p) = 0, \text{Re}(p) > 0$ are introduced for $\sqrt{\pm p}$, respectively, such that $\text{Re}(\sqrt{\pm p}) > 0$ in the cut p -plane. Behavior of (B_5, A_{\pm}) therefore helps to define allowable speed for a particular solid.

Transform inversion — transversely isotropic solid, allowable speed

In view of [Payton 1983] and (4b), transversely isotropic solids can be categorized as follows, where we define $\gamma = 1 + d_1 d_2 - (1 + d_{12})^2$:

θ	0°	30°	45°	60°	90°
$c_+(\theta)$	2.0564	1.9502	1.8149	1.6673	1.2762
$c_-(\theta)$	1.0	0.8805	0.7967	0.7061	1.0
$c_5(\theta)$	1.2823	1.2178	1.1498	1.0775	1.0

Table 1. Dimensionless speeds for x_V -direction in x_1x_2 -principal plane (zinc).

$$\begin{aligned}
 \text{I:} & \quad \begin{cases} 2\sqrt{d_1d_2} \leq \gamma \leq 1 + d_1d_2 & \text{for } 1 < d_1 < d_2, \\ d_1 + d_2 \leq \gamma \leq 1 + d_1d_2 & \text{for } 1 < d_2 < d_1, \\ 2d \leq \gamma \leq 1 + d^2 & \text{for } 1 < d_1 = d_2 = d; \end{cases} \\
 \text{II:} & \quad 1 + d_1 < \gamma < d_1 + d_2 \quad \text{for } \gamma^2 - 4d_1d_2 < 0; \\
 \text{III:} & \quad \gamma < 1 + d_1 \quad \text{for } \gamma^2 - 4d_1d_2 < 0.
 \end{aligned}$$

For $|\psi - \theta| < \pi/2$ and $M^2 - 4d_1C_2C_0 \geq 0$ Equations (13c) and (13d) hold, and A_{\pm} is real and nonnegative. For $M^2 - 4d_1C_2C_0 \leq 0$ however, the complex conjugates arise:

$$A_{\pm} = \Omega_C \pm i\Omega_S, \tag{14a}$$

$$\Omega_C = \frac{1}{\sqrt{2}}\sqrt{A_{\Psi}^2 + \cos^2 \psi + M/2d_1} \geq 0, \quad \Omega_S = \frac{1}{\sqrt{2}}\sqrt{A_{\Psi}^2 - \cos^2 \psi - M/2d_1} \geq 0, \tag{14b}$$

$$A_{\Psi} = [\cos^4 \psi + (M \cos^2 \psi + C_2C_0)/d_1]^{1/4}, \tag{14c}$$

$$A_+ + A_- = 2\Omega_C, \quad A_+A_- = A_{\Psi}^2. \tag{14d}$$

For $|\psi - \theta| < \frac{\pi}{2}$, $c_V < c$ so that allowable speed for a given translation direction is defined by branch points of (A_{\pm}, B_5) on the positive $\text{Re}(c)$ -axis for $(\psi = \theta, |\theta| < \frac{\pi}{2})$:

$$c_{\pm}(\theta) = \sqrt{D_2 \pm \sqrt{D_2^2 - D_4}}, \quad c_5(\theta) = \sqrt{d_5 \cos^2 \theta + \sin^2 \theta}, \tag{15a}$$

$$D_2 = \frac{1}{2}(1 + d_1 \cos^2 \theta + d_2 \sin^2 \theta), \tag{15b}$$

$$D_4 = d_1 \cos^4 \theta + d_2 \sin^4 \theta + \gamma \sin^2 \theta \cos^2 \theta. \tag{15c}$$

As an illustration, consider materials [Payton 1979]

III (zinc): $d_1 = 4.2286, d_2 = 1.6286, d_5 = 1.6442, d_{12} = 1.3195, d_{13} = 0.9403$.

I (beryl): $d_1 = 4.11, d_2 = 3.62, d_5 = 2.0, d_{12} = 1.017, d_{13} = 1.055$.

Calculations of (15a) are presented in Tables 1 and 2 for values of θ . Table 1 for zinc demonstrates that $c_+(\theta) > c_5(\theta) \geq c_-(\theta)$. Table 2, however, shows that the relation between $c_5(\theta)$ and $c_-(\theta)$ is itself θ -dependent. Although these are examples, the present study will focus on category III materials and, in particular, those which, like zinc, restrict speed for translation direction $|\theta - \psi| < \frac{\pi}{2}$ to the range $0 < c < c_-(\theta)$.

In view of this, and conditions on contour function \mathfrak{S} , (10) assumes the form

$$\frac{1}{i\pi} \int_{\Psi} P_k d\psi \int_N d\eta \frac{\partial}{\partial x} \int_X d\xi \frac{\partial U_k}{\partial \xi}(\xi, \eta) \frac{1}{2\pi i} \int \frac{|p| \sqrt{-p}}{p \sqrt{p}} dp \exp(p(x - \xi)). \tag{16}$$

θ	0°	30°	45°	60°	90°
$c_+(\theta)$	2.0278	1.9428	1.857	1.8514	1.9026
$c_-(\theta)$	1.0	1.1326	1.1902	1.1469	1.0
$c_5(\theta)$	$\sqrt{2}$	1.3229	1.2247	1.118	1.0

Table 2. Dimensionless speeds for x_V -direction in x_1x_2 -principal plane (beryl).

Symbols (N, X, Ψ) signify integration over ranges $|\psi - \theta| < \frac{\pi}{2}$, $N^- < \eta < N^+$ and $X_- < \xi < X_+$, respectively. In light of (A.1), (13d) and (14d), term $P_k = P_k(\psi, \theta)$ is real-valued. The p -integration is along the positive side of the entire imaginary axis, and can be performed by use of Appendix B. Then, because U_k vanishes continuously on C , (16) gives

$$\frac{1}{\pi} \int_{\Psi} P_k d\psi \frac{\partial}{\partial x} \int_N d\eta \frac{1}{\pi} \int_X \frac{\partial U_k}{\partial \xi}(\xi, \eta) \frac{d\xi}{\xi - x}. \tag{17}$$

Limits $N^\pm(\psi)$ in (17) are defined by

$$\Im(\xi_1(\xi, N^\pm), \xi_2(\xi, N^\pm)) = 0, \quad \frac{dN^\pm}{d\xi} = 0. \tag{18}$$

That is, for given ψ , limits N^\pm are the maximum and minimum values of η on B_C , and for given η , limits $X_\pm(\psi, \eta)$ locate the ends of lines that run parallel to the ξ -axis and that span A_C . Conditions on B_C imply that these limits exist, are single-valued, and vary continuously in ψ . Figure 1 gives a generic sketch for A_C and it is seen that, for semi-infinite A_C , $N^\pm(\psi) \rightarrow \pm\infty$ and $|X_-(\psi, \eta)| \rightarrow \infty$ for certain ranges of ψ .

In light of (7)–(12), traction in A_C itself, i.e., $x_3 = 0$, $(x_1, x_2) \in A_C$, is

$$\sigma_{3k} = -\frac{1}{\pi} \int_{\Psi} d\psi \int_N d\eta \frac{\partial}{\partial x} \int_X d\xi \delta(\xi, \eta) \sigma_{3k}(x_1(\xi, \eta), x_2(\xi, \eta)). \tag{19}$$

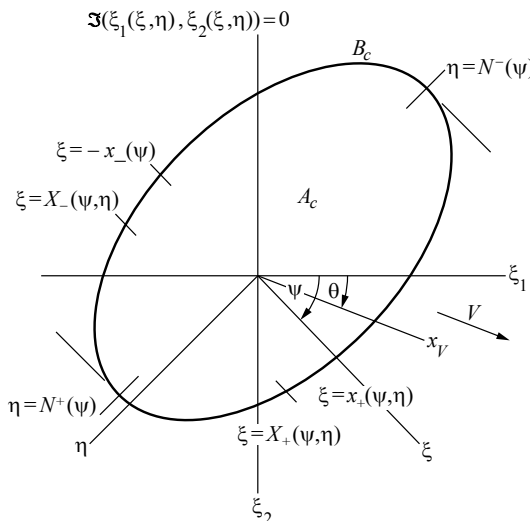


Figure 1. Schematic of area A_C and contour B_C .

In (19), δ is the Dirac function. Therefore, expressions for traction in A_C can be obtained by matching the integrands of (ψ, η) -integration in (19) with combinations of those in (17). Moreover, ξ in (17) and (19) is an integration variable representing parameter x that itself depends on (x_1, x_2) and ψ . As noted in connection with (11), coordinates (x_1, x_2) can be replaced by (x, ψ) for $y = 0$. Thus, every point $(x_1, x_2) \in A_C$ lies on an integration path $\eta = 0$ that passes through both limit points of the ξ -integral. Results of matching (17) and (19) give, therefore, expression (C.3).

Related crack growth problem: Basic results

Region A_C is now a semi-infinite crack, i.e., translation speed V is the crack growth speed, and $\Im(x_1, x_2) = 0$ is such that B_C in Figure 1 is an arc of infinite length. The two crack surfaces are subjected to equal compressive stress $\sigma_{32} = \sigma_{31} = 0$, $\sigma_{33} = -\sigma_{33}^C$, where, for $(x_1, x_2) \in A_C$, σ_{33}^C is nonnegative, finite, piecewise continuous and

$$\sigma_{33}^C \approx O((x_1^2 + x_2^2)^{-\chi}), \quad \sqrt{x_1^2 + x_2^2} \rightarrow \infty \quad \text{for } \chi > 1. \quad (20)$$

Coupled singular integral equations for the x -derivatives of (U_1, U_2, U_3) are provided by (C.3), with $(\sigma_{32}, \sigma_{31}) = 0$ and $\sigma_{33} = -\sigma_{33}^C$. Solution gives the derivatives and the functions themselves. If σ_{33}^C -values are largest near $(x_1, x_2) = 0$, it is reasonable to assume that any curvature of crack edge B_C will produce an essentially concave profile with respect to this point. In view of the original conditions on B_C then, $(U_1, U_2) = 0$ and two cases arise for U_3 . Case $X_+ = x_+(\psi) > 0$, $X_- = -x_-(\psi)$ gives

$$\frac{\partial U_3}{\partial x} = \frac{1}{\sqrt{x_+ - x} \sqrt{x + x_-}} \frac{(vp)}{\pi} \int_X \frac{g_3 d\xi}{\xi - x} \sqrt{x_+ - \xi} \sqrt{\xi + x_-}, \quad (21a)$$

$$U_3 = \frac{1}{\pi} \int_X g_3 d\xi \ln \left| \frac{\sqrt{x_+ - x} \sqrt{\xi + x_-} - \sqrt{x + x_-} \sqrt{x_+ - \xi}}{\sqrt{x_+ - x} \sqrt{\xi + x_-} + \sqrt{x + x_-} \sqrt{x_+ - \xi}} \right|, \quad (21b)$$

$$g_3 = -\frac{2C_0}{\mu G_3} \sigma_{33}^C. \quad (21c)$$

Continuity of B_C requires $x_{\pm}(\frac{\pi}{2} - \theta) = x_{\mp}(-\frac{\pi}{2} - \theta)$. For $X_+ = x_+(\psi)$, $X_- \rightarrow -\infty$,

$$\frac{\partial U_3}{\partial x} = \frac{1}{\sqrt{x_+ - x}} \frac{(vp)}{\pi} \int_X \frac{g_3 d\xi}{\xi - x} \sqrt{x_+ - \xi}, \quad (22a)$$

$$U_3 = \frac{1}{\pi} \int_X g_3 d\xi \ln \left| \frac{\sqrt{x_+ - \xi} - \sqrt{x_+ - x}}{\sqrt{x_+ - \xi} + \sqrt{x_+ - x}} \right|. \quad (22b)$$

Continuity of B_C now requires that $x_+(\theta \pm \frac{\pi}{2}) \rightarrow \infty$. Equations (21b) and (22b), as is appropriate, vanish continuously on B_C . Substitution of (21a) and (22a) into (17) and performing the ξ -integration for $x \notin X$ leads to, respectively, expressions for traction on plane $x_3 = 0$, $(x, \psi) \notin A_C$:

$$\sigma_{33} = \frac{1}{\pi \sqrt{x_+ - x} \sqrt{x_- + x}} \int_X \frac{\sigma_{33}^C d\xi}{\xi - x} \sqrt{x_+ - \xi} \sqrt{\xi + x_-}, \quad (23a)$$

$$\sigma_{33} = \frac{1}{\pi \sqrt{x_+ - x}} \int_X \frac{\sigma_{33}^C d\xi}{\xi - x} \sqrt{x_+ - \xi}. \quad (23b)$$

Critical speed: Illustration

Restriction $0 < c < c_-(\theta)$ guarantees a bounded solution. In addition, (21b) and (22b) define crack surface separation, which should be nonnegative. Thus term C_0/G_3 in (21c) should be negative and finite. The same condition arises in the isotropic limit

$$d_1 = d_2 = d, \quad d_4 = d_5 = 1, \quad d_{12} = d_{13} = d - 2, \quad d = 2 \frac{1 - \nu}{1 - 2\nu}.$$

Here ν is Poisson’s ratio, and it can be shown that

$$c_+(\theta) = \sqrt{d}, \quad c_-(\theta) = c_5(\theta) = 1, \tag{24a}$$

$$A_+ = A = \sqrt{1 - c_V^2/d}, \quad A_- = B_5 = B = \sqrt{1 - c_V^2}, \tag{24b}$$

$$G_3/C_0 = -R/c_V^2 A, \quad R = 4AB - (1 + B^2)^2. \tag{24c}$$

In (24c), $R \rightarrow 0+$ ($c_V \rightarrow 0$) and $R = -1$ ($c_V \rightarrow 1$), which implies that $R = 0$ ($c_V = c_R$, $0 < c_R < 1$). Thus, R is a Rayleigh function, V_R is the Rayleigh speed, and crack growth rate is restricted by $0 < c < c_R$.

The situation is more complicated for the transversely isotropic solid: for $\psi = \theta = 0$, G_3/C_0 is negative for $c < c_-$ and vanishes when

$$4A_1A_5 - (1 + A_5^2)^2 = 0, \tag{25a}$$

$$A_1 = \sqrt{1 - c^2/d_1}, \quad A_5 = \sqrt{1 - c^2/d_5}. \tag{25b}$$

For the category III solid, in particular, G_3/C_0 vanishes for $\psi = \theta = \frac{\pi}{2}$ when

$$\left[1 + (1 + d_{12})^2 - \sqrt{d_1 d_2} A_2 B\right] B^2 + \sqrt{d_1 d_2} (1 - \sqrt{d_1 d_2} B^2) A_2^2 = 0, \tag{26a}$$

$$A_2 = \sqrt{1 - c^2/d_2}, \quad B = \sqrt{1 - c^2}. \tag{26b}$$

Calculations for zinc give the roots of (25a) and (26a) as $c_R \approx 1.16$ and $c_R \approx 0.26$, respectively. However, Table 1 shows that the first root exceeds $c_-(0)$. A similar result arose for sliding contact [Brock 2013]. That is, G_3/C_0 plays the role of a Rayleigh function (cf. (25a) and (24c)) but its roots c_R may not give the minimum critical speed.

Brittle fracture parameter: Energy release (rate)

After [Griffith 1921] crack growth occurs when the rate of dynamic energy release matches that of potential energy decrease. For the 2D brittle crack, this criterion equates the rate per unit length (of crack edge) of energy release and negative of power per unit length generated in the crack plane [Willis 1971; Achenbach 1973; Freund 1990]. Here, total release rate \dot{D}_3 and total power are considered. Affixed subscript “3” signifies the possibility that release rate in an anisotropic material depends on orientation of the fracture surface, e.g., here the surface normal aligns with the x_3 -principal direction. Use of (8) for the dynamic steady state gives

$$\dot{D}_3 = -V \int_{\Psi} d\psi \left[\left(\int_{-\infty}^{\infty} - \int_X \right) dx \sigma_{33} \partial_V U_3 + \int_X |x| dx \sigma_{33}^C \partial_V U_3 \right], \tag{27a}$$

$$\partial_V = \cos(\psi - \theta) \frac{\partial}{\partial x} - \frac{\sin(\psi - \theta)}{|x|} \frac{\partial}{\partial \psi}. \quad (27b)$$

To illustrate the form of \dot{D}_3 the ∂_V -operator is applied to case (23b):

$$\begin{aligned} \partial_V U_3 = & -\frac{(vp)}{\pi \sqrt{x_+ - x}} \int_X g_3 d\xi \left[\frac{\sqrt{x_+ - \xi}}{\xi - x} \cos(\psi - \theta) - \frac{\sin(\psi - \theta)}{|x| \sqrt{x_+ - \psi}} \frac{dx_+}{d\psi} \right] \\ & + \frac{\sin(\psi - \theta)}{\pi |x|} \int_X d\xi \ln \left| \frac{\sqrt{x_+ - \xi} + \sqrt{x_+ - x}}{\sqrt{x_+ - \xi} - \sqrt{x_+ - x}} \right| \frac{\partial g_3}{\partial \psi}. \end{aligned} \quad (28)$$

Equations (5a), (23b) and (28) imply that $\dot{D}_3 = 0$ in (27a). However (23b) and (28) are square-root singular for $x \rightarrow x_+ + 0$ and $x \rightarrow x_+ - 0$ respectively and, in the sense of a distribution [Achenbach and Brock 1973],

$$\frac{H(x_+ - x)}{\sqrt{x_+ - x}} \frac{H(x - x_+)}{\sqrt{x - x_+}} = \frac{\pi}{2} \delta(x - x_+). \quad (29)$$

Here H is the step function. Also, \dot{D}_3 is assumed invariant in (27a) with respect to its integrand. Singular behavior guarantees invariance in terms of x , so that the integrand need only be constant in terms of ψ . Therefore, for $|\psi - \theta| < \frac{\pi}{2}$,

$$\frac{\dot{D}_3}{\mu V_S} = -\frac{cC_0}{G_3} \left(\frac{G}{\mu} \right)^2 \frac{d}{d\psi} [x_+ \sin(\psi - \theta)], \quad G = \int_X \frac{\sigma_{33}^C dt}{\sqrt{x_+ - t}}. \quad (30)$$

Equation (30) is a nonlinear differential equation for $x_+(\psi)$ based on (23), i.e., semi-infinite A_C .

Illustration: Point force

Consider compressive point force loading

$$\sigma_{31}^C = \sigma_{32}^C = 0, \quad \sigma_{33}^C = \frac{P \delta(r_0)}{2\pi r_0}, \quad r_0 = \sqrt{x_1^2 + x_2^2}. \quad (31)$$

Here P is a force, so that traction σ_{33}^C is the axially symmetric Dirac function in standard polar coordinates. Function G in (30) for (31) is given in Appendix D. The right-hand side of (30) must be finite for $|\psi - \theta| \rightarrow \frac{\pi}{2}$, and use of (13a), (C.2d) and (D.4b) gives

$$x_+ \approx \sqrt{\frac{c}{2S} \frac{\mu V_S}{\dot{D}_3} \frac{P}{2\pi \mu} \frac{1}{\sqrt{\cos(\psi - \theta)}}} \quad \text{as } |\psi - \theta| \rightarrow \frac{\pi}{2}. \quad (32)$$

Terms in (32) are given by

$$S = 4d_5 c'_5 \tan^2 \theta + \frac{Q}{\Omega} \sqrt{d_1} \cos^2 \theta + T'^2 \left(\frac{Q}{\Omega} \sqrt{d_1} - \frac{\Omega}{D_4} \right), \quad (33a)$$

$$c'_5 = \sqrt{d_5 \sin^2 \theta + \cos^2 \theta}, \quad (33b)$$

$$Q = 1 + \frac{1}{D_4} \left(\sqrt{d_1} \sin^2 \theta + \frac{\cos^2 \theta}{\sqrt{d_1}} \right), \quad T' = \frac{2c'_5{}^2}{\cos \theta} - \cos \theta, \quad (33c)$$

$$\Omega = \sqrt{\gamma \cos^2 \theta + 2\sqrt{d_1}(\sqrt{d_1} \sin^2 \theta + D_4)}, \tag{33d}$$

$$D_4 = \sqrt{d_1 \sin^4 \theta + d_2 \cos^4 \theta + \gamma \sin^2 \theta \cos^2 \theta}. \tag{33e}$$

Equation (30) involves only $x_+(\theta)$ itself for $\psi = \theta$, i.e., the distance between point forces and crack edge measured in the direction of translation. In light of Appendix D, (30) can be solved algebraically as

$$x_+(\theta) = F(c, \theta)L, \tag{34a}$$

$$F(c, \theta) = \sqrt{-cC_0/G_3}, \quad L = (P/2\pi)\sqrt{V_S/\mu\dot{D}_3}. \tag{34b}$$

Reference length L depends on a force/energy ratio. Term $F(c, \theta)$ is dimensionless. Quantities (C_0, G_3) come from (13), (14), (C.2d) and (C.3b) upon setting $\psi = \theta$, $c_V = c$. In view of (34) and invariance, (30) can be rewritten for $|x - \theta| < \frac{\pi}{2}$ as

$$-\frac{2C_0}{G_3x_+^3} \frac{d}{d\psi} [\sin(\psi - \theta)x_+] = \frac{F^2(c, \theta)}{cx_+^2(\theta)}. \tag{35}$$

On the left-hand side of (35) we temporarily introduce $z = x_+ \sin(\psi - \theta)$, which allows separation of variables. Integration in view of the asymptotic behavior noted above then gives x_+ when $\psi \neq \theta$:

$$\frac{x_+^2(\theta)}{x_+^2(\psi)} = \frac{1}{c} F^2(c, \theta) \sin^2(\psi - \theta) \int_- \frac{G_3 d\phi}{C_0 \sin^3(\phi - \theta)} \quad \text{for } -\frac{\pi}{2} < \psi - \theta < 0, \tag{36a}$$

$$\frac{x_+^2(\theta)}{x_+^2(\psi)} = -\frac{1}{c} F^2(c, \theta) \sin^2(\psi - \theta) \int_+ \frac{G_3 d\phi}{C_0 \sin^3(\phi - \theta)} \quad \text{for } 0 < \psi - \theta < \frac{\pi}{2}. \tag{36b}$$

Symbols \pm affixed to integral operators in (36) signify, respectively, integration ranges $\psi < \phi < \theta + \frac{\pi}{2}$ and $\theta - \frac{\pi}{2} < \phi < \psi$. Differentiation of (36) shows that $dx_+/d\psi = 0$ for $\psi = \theta$, i.e., crack edge and direction of point force translation are perpendicular directly ahead of the forces.

Calculations

Equation (36) and the asymptotic behavior noted for (32) indicate that, as in the isotropic case [Brock 2015], the crack edge B_C resembles those in Figure 2, where “x” denotes point force location. That is, it is a straight line at right angles to the translation/growth direction that is deformed by a bulge near the location $x = 0$ of the translating point forces. Bulge size is characterized somewhat by the distance $x_+(\theta)$ in (34). Therefore, values of dimensionless ratio $F(c, \theta)$ are displayed in Table 3 for $\theta = (0^\circ, 30^\circ, 45^\circ, 60^\circ, 90^\circ)$ respectively, and subcritical values of c . Entries in Table 3 show that the bulge effect is enhanced by increase in extension speed (c) and by deviation (θ) in force translation direction from the x_1 -principal direction. Perhaps the latter behavior arises because $d_2 < d_1$ ($C_{22} < C_{11}$).

Some observations for more general loading

Consider in place of (31) a finite, simply connected region $A_0 \in A_C$ subjected to a finite and piecewise continuous pressure p_0 . The Green’s function for this case is obtained by replacing $(P, |x|)$ in (D.2)

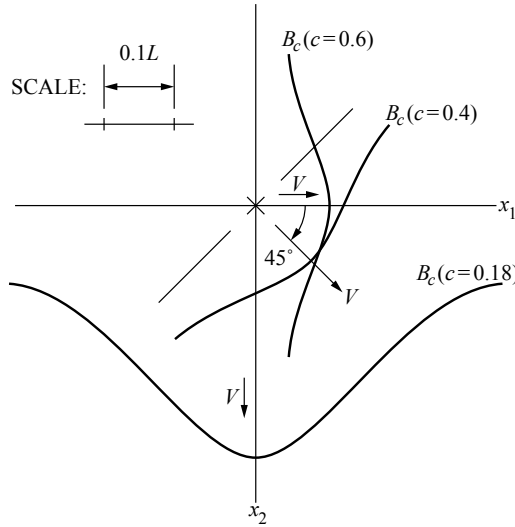


Figure 2. Sketches of crack edge contour B_C .

with, respectively,

$$\iint_{A_0} p_0(u, \phi) |u| \, du \, d\phi, \tag{37a}$$

$$X = \sqrt{x^2 + u^2 - 2ux \cos(\phi - \psi)}. \tag{37b}$$

Quasipolar coordinates (u, ϕ) lie in A_0 and, in consequence, the right-hand side of (D.3) is

$$\frac{1}{\sqrt{z - x_+ Z}} \frac{1}{Z^2 + \epsilon^2}, \quad Z = \sqrt{z^2 + u^2 - 2uz \cos(\phi - \psi)}. \tag{38a}$$

Now $F_G(z)$ has three nonintersecting branch cuts, and the right-hand side of (D.4b) is

$$\iint_{A_0} \frac{d\phi}{\pi \sqrt{2}} \frac{p_0(u, \phi) |u| \, du}{Z_+ \sqrt{Z_+ + x_+ - u \cos(\phi - \psi)}} \quad \text{as } \epsilon \rightarrow 0, \tag{38b}$$

$$Z_+ = \sqrt{x_+^2 + u^2 - 2ux_+ \cos(\phi - \psi)}. \tag{38c}$$

Use of (38b) gives an equation for $x_+(\theta)$ that in general does not yield a closed-form result such as (34a). The result for x_+ when $|\psi - \theta| \rightarrow \frac{\pi}{2}$, however, is given by (32) with P replaced by (37a). That is, asymptotic behavior of the crack edge depends only on total compressive load, not how that load may be distributed over a finite area.

	$c = 0.1$	$c = 0.2$	$c = 0.3$	$c = 0.4$
$\theta = 0^\circ$	0.03559	0.05069	0.06286	0.07394
$\theta = 30^\circ$	0.04288	0.06169	0.07773	0.09402
$\theta = 45^\circ$	0.02526	0.0687	0.0883	0.112
$\theta = 60^\circ$	0.0538	0.07902	0.1043	0.14
$\theta = 90^\circ$	0.1439	0.2473	$c > c_R$	$c > c_R$

Table 3. Crack edge location parameter $F(c, \theta)$ (zinc).

Some comments

This study extends a dynamic steady-state 3D analysis for an isotropic solid [Brock 2015] by illustrating semi-infinite crack growth in the principal plane of a transversely isotropic solid. Fracture is driven by compressive traction applied to the crack surfaces. An exact solution is possible and, upon introduction of a quasipolar coordinate system, gives a nonlinear first-order differential equation for the distance between a point on the crack plane and the crack edge. The distance function therefore defines the crack contour. The equation is studied for point force loading, so that distance can be chosen as that between forces and crack edge. Calculations show that the crack edge is rectilinear away from the point forces, and translates with them. Near the point forces, however, a bulge forms about them. Force-crack edge distance now increases with force translation speed, and increases are even more prominent as the translation direction aligns with the principal axis associated with the smaller elastic modulus.

These results are consistent with those of [Brock 2015]. Calculations of the distance (contour) function, however, require numerical evaluation of first integrals in (36); in [Brock 2015] analytical evaluation is possible. In addition these results are illustrations for a particular category of transversely isotropic solids [Payton 1983]. Nevertheless, general effects of transverse isotropy are emphasized, because the axis of material symmetry lies in the crack plane. These results are also consistent with those for sliding indentation on a half-space whose surface is the same principal plane [Brock 2013]: minimum critical growth rate may not be a Rayleigh speed. In closing, however, it should be mentioned that the possibility of energy release (rate) dependence on crack surface orientation was not exploited here.

Appendix A

For $x_3 = 0$:

$$\frac{\Gamma_0}{\mu} \hat{\sigma}_{33} = \hat{U}_3 \left[2d_5^2 p_1^2 B_5 + \frac{(\Gamma_1 - A_+ A_-)}{2A_+ A_- (A_+ + A_-)} (\frac{1}{2} T_5^2 + \Gamma_0 p_2^2) + \frac{1}{2} T_5^2 \left(\frac{1}{A_+} + \frac{1}{A_-} \right) \right], \tag{A.1a}$$

$$\frac{\Gamma_0}{\mu} \hat{\sigma}_{31} = \frac{T_5}{2B_5} (T_5 \hat{U}_1 + p_1 p_2 \hat{U}_2) + \frac{d_5 p_1}{A_+ + A_-} \left[(\Gamma_1 - A_+ A_-) (2p_1 \hat{U}_1 - p_2 \hat{U}_2) - \frac{\Gamma_0 p_2 \hat{U}_2}{d_1 (1 + d_{12})} \right], \tag{A.1b}$$

$$\begin{aligned} \frac{\Gamma_0}{\mu} \hat{\sigma}_{32} = & \frac{p_1 p_2}{2B_5} (T_5 \hat{U}_1 + p_1 p_2 \hat{U}_2) - \Gamma_0 \left[\frac{d_5 (1 + d_{12}) p_1 p_2}{A_+ + A_-} \hat{U}_1 + \frac{1}{2} \hat{U}_2 (A_+ + A_-) \right] \\ & - \frac{\Gamma_1 - A_+ A_-}{A_+ + A_-} [d_5 p_1 p_2 \hat{U}_1 + (p_2^2 + \Gamma_0) \frac{1}{2} \hat{U}_2]. \end{aligned} \tag{A.1c}$$

Appendix B

Consider the integral over the entire $\text{Im}(p)$ -axis:

$$\frac{1}{2\pi i} \int |p| \frac{\sqrt{-p}}{\sqrt{p}} (A_R \mp i A_I) \exp(pX - (Y_R \mp i Y_I) \sqrt{-p} \sqrt{p}) \frac{dp}{p}. \tag{B.1}$$

Here (A_R, A_I, X, Y_R, Y_I) are real constants, with $(X, Y_R, Y_I) \geq 0$, and \mp signifies, respectively, $\text{Im}(p) > 0$ and $\text{Im}(p) < 0$. As noted in connection with (11) and (12), $\text{Re}(\sqrt{\pm p}) \geq 0$ in the p -plane with branch cuts $\text{Im}(p) = 0, \text{Re}(p) < 0$ and $\text{Im}(p) = 0, \text{Re}(p) > 0$, respectively. In particular, for $\text{Re}(p) = 0+$ and,

respectively, $\text{Im}(p) = q > 0$ and $\text{Im}(p) = q < 0$, we have

$$\sqrt{-p} = \left| \frac{q}{2} \right|^{1/2} (1 \mp i), \quad \sqrt{p} = \left| \frac{q}{2} \right|^{1/2} (1 \pm i). \quad (\text{B.2})$$

Use of (B.2) reduces (B.1) to

$$\frac{1}{i\pi} \int_0^\infty \exp(-Y_R q) [A_R \cos(X + Y_I)q - A_I \sin(X + Y_I)q] dq. \quad (\text{B.3})$$

Performing the integration gives

$$\frac{1}{i\pi} \left[A_R \frac{X + Y_I}{(X + Y_I)^2 + Y_R^2} - A_I \frac{Y_R}{(X + Y_I)^2 + Y_R^2} \right]. \quad (\text{B.4a})$$

If factor $\sqrt{-p}/\sqrt{p}$ in (B.1) is replaced by unity, the result becomes

$$\frac{1}{i\pi} \left[A_R \frac{Y_R}{(X + Y_I)^2 + Y_R^2} + A_I \frac{X + Y_I}{(X + Y_I)^2 + Y_R^2} \right]. \quad (\text{B.4b})$$

It is noted that

$$\frac{1}{\pi} \frac{Y_R}{(X + Y_I)^2 + Y_R^2} \rightarrow \delta(X + Y_I) \quad \text{as } Y_R \rightarrow 0+. \quad (\text{B.5})$$

Here δ is the Dirac function.

Appendix C

For $x_3 = 0$, $X_- < x < X_+$, $\psi \in \Psi$, i.e., $x_3 = 0$, $(x_1, x_2) \in C$, we have

$$\sigma_{33} = -\frac{\mu}{2\pi C_0} (vp) \int_X \frac{\partial U_3}{\partial x} \frac{G_3 d\xi}{\xi - x}, \quad (\text{C.1a})$$

$$\sigma_{31} = -\frac{\mu}{2\pi C_0} (vp) \int_X \frac{\partial U_1}{\partial x} \frac{G_1 d\xi}{\xi - x} - \frac{\mu}{2\pi C_0} (vp) \int_X \frac{\partial U_2}{\partial x} \sin 2\psi \frac{G_{12} d\xi}{\xi - x}, \quad (\text{C.1b})$$

$$\sigma_{32} = -\frac{\mu}{2\pi C_0} (vp) \int_X \frac{\partial U_1}{\partial x} \sin 2\psi \frac{G_{21} d\xi}{\xi - x} - \frac{\mu}{2\pi C_0} (vp) \int_X \frac{\partial U_2}{\partial x} \frac{G_2 d\xi}{\xi - x}. \quad (\text{C.1c})$$

Here $U_k = U_k(\xi, \psi)$, (vp) signifies the principal value, and for $M^2 - 4d_1 C_2 C_0 > 0$ we have

$$G_1 = -\frac{T_5^2}{B_5} - 4d_5 \frac{A_+ A_- + C_1}{A_+ + A_-} \cos^2 \psi, \quad (\text{C.2a})$$

$$G_2 = -\frac{\sin^2 2\psi}{2B_5} - C_0(A_+ + A_-) + \frac{A_+ A_- + C_1}{A_+ + A_-} (\sin^2 \psi - C_0), \quad (\text{C.2b})$$

$$G_{12} = G_{21} = -\frac{T_5}{2B_5} + \frac{2d_5}{A_+ + A_-} \left[A_+ A_- + C_1 + (1 + d_{12}) \frac{C_0}{d_1} \right], \quad (\text{C.2c})$$

$$G_3 = 4d_5^2 B_5 \cos^2 \psi + \left(1 + \frac{C_1}{A_+ A_-} \right) \frac{T_5^2 + C_0 \sin^2 \psi}{A_+ + A_-} - \frac{T_5^2}{A_+ A_-} (A_+ + A_-). \quad (\text{C.2d})$$

For $M^2 - 4d_1 C_2 C_0 < 0$ we have

$$G_1 = -\frac{T_5^2}{B_5} - \frac{2d_5}{\Omega_C} (A_\Psi^2 + C_1) \cos^2 \psi, \quad (\text{C.3a})$$

$$G_2 = -\frac{\sin^2 2\psi}{2B_5} - 2C_0 \Omega_C + \frac{1}{2\Omega_C} (A_\Psi^2 + C_1) (\sin^2 \psi - C_0), \quad (\text{C.3b})$$

$$G_{12} = G_{21} = -\frac{T_5}{2B_5} + \frac{d_5}{\Omega_C} \left[A_\Psi^2 + C_1 + (1 + d_{12}) \frac{C_0}{d_1} \right], \quad (\text{C.3c})$$

$$G_3 = 4d_5^2 B_5 \cos^2 \psi + \frac{1}{2\Omega_C} \left(1 + \frac{C_1}{A_\Psi^2} \right) (T_5^2 + C_0 \sin^2 \psi) - \frac{2\Omega_C}{A_\Psi^2} T_5^2. \quad (\text{C.3d})$$

Equations (13) and (14) govern equations (C.2) and (C.3), respectively. Term C_0 defined by (13a) may vanish for subcritical V , but ratios of $(G_1, G_2, G_{12}, G_{21}, G_3)$ with C_0 remain finite, e.g., for $c_V^2 \rightarrow \sin^2 \psi$

$$\begin{aligned} \frac{G_3}{C_0} &= 2d_5 \cos^2 \psi + \frac{1}{M_C} (4d_5^2 \cos^2 \psi + \sin^2 \psi) + 4d_5^2 \cos^2 \psi \left[\frac{\cos \psi}{d_1 M_C (M_C + \cos \psi)} - \frac{1}{M_C} - \frac{1}{\cos \psi} \right] \\ &\quad - \frac{d_5^2}{d_1 M_C} \cos^3 \psi (m_+ \cos \psi + m_- M_C) \left[1 + \frac{1 + \cos \psi}{M_C (M_C + \cos \psi)} \right], \end{aligned} \quad (\text{C.4a})$$

$$m_+ = 1 + d_1 + (1 + d_{12})^2, \quad m_- = \sin^2 \psi - \frac{2d_1(d_2 - 1)}{\gamma - 1 - d_1}, \quad (\text{C.4b})$$

$$M_C = \sqrt{\cos^2 \psi + \left[\frac{1}{d_1} (\gamma - 1) - 1 \right] \sin^2 \psi}, \quad (\text{C.4c})$$

$$\gamma = 1 + d_1 d_2 - (1 + d_{12})^2. \quad (\text{C.4d})$$

Appendix D

In terms of quasipolar coordinates (x, ψ) , (31) gives

$$\sigma_{33}^C = P \frac{\delta(x)}{\pi |x|}, \quad |\psi| < \frac{\pi}{2}. \quad (\text{D.1})$$

Evaluation of G in (30) is obtained in terms of representation

$$\sigma_{33}^C = P \frac{\epsilon}{\pi^2 |x| (x^2 + \epsilon^2)} \quad \text{as } \epsilon \rightarrow 0. \quad (\text{D.2})$$

Function $F_G(z)$ in the complex z -plane, where $x = \text{Re}(z)$, is defined as

$$F_G(z) = \frac{1}{\sqrt{z^2 - \epsilon_0^2} (z^2 + \epsilon^2) \sqrt{z - x_+}} \quad \text{for } \epsilon_0 \approx 0. \quad (\text{D.3})$$

Here $F_G \approx O(z^{-3})$, $|z| \rightarrow \infty$ and exhibits branch cuts on the $\text{Re}(z)$ -axis with branch points $z = (\pm\epsilon_0, x_+)$, and poles $z = \pm i\epsilon$. Thus integration over a closed contour that includes a portion $|z| \rightarrow \infty$, but excludes the poles and branch cuts, can be performed by residue theory. Setting $\epsilon_0 = 0$ then leads to the following expressions for G :

$$G = \frac{P}{\pi\alpha\sqrt{2(1+\alpha)}} \frac{1}{x_+^{3/2}}, \quad \alpha = \sqrt{1 + \epsilon^2/x_+^2}, \quad (\text{D.4a})$$

$$G = \frac{P}{2\pi x_+^{3/2}} \quad \text{as } \epsilon \rightarrow 0. \quad (\text{D.4b})$$

References

- [Achenbach 1973] J. D. Achenbach, *Wave propagation in elastic solids*, Applied Mathematics and Mechanics **16**, North-Holland, Amsterdam, 1973.
- [Achenbach and Brock 1973] J. D. Achenbach and L. M. Brock, “On quasistatic and dynamic fracture”, pp. 529–541 in *Proceedings of an international conference on dynamic crack propagation*, edited by G. C. Sih, Springer, Netherlands, 1973.
- [Barber 1992] J. R. Barber, *Elasticity*, Solid Mechanics and its Applications **12**, Kluwer, Dordrecht, 1992.
- [Brock 2013] L. M. Brock, “Rapid sliding contact in three-dimensional by an ellipsoidal die on transversely isotropic half-spaces with surfaces on different principal planes”, *J. Appl. Mech. (ASME)* **81**:3 (2013), Art. ID #031005.
- [Brock 2015] L. M. Brock, “Contours for planar cracks in three dimensions”, *J. Mech. Mater. Struct.* **10**:1 (2015), 63–77.
- [Freund 1990] L. B. Freund, *Dynamic fracture mechanics*, Cambridge University Press, 1990.
- [Griffith 1921] A. A. Griffith, “The phenomena of rupture and flow in solids”, *Phil. Trans. R. Soc. A* **221**:582–593 (1921), 163–198.
- [Jones 1999] R. M. Jones, *Mechanics of composite materials*, 2nd ed., Taylor & Francis, New York, 1999.
- [Payton 1979] R. G. Payton, “Epicenter motion of a transversely isotropic elastic half-space due to a suddenly applied buried point source”, *Int. J. Eng. Sci.* **17**:7 (1979), 879–887.
- [Payton 1983] R. G. Payton, *Elastic wave propagation in transversely isotropic media*, Mechanics of elastic and inelastic solids **4**, Kluwer, The Hague, 1983.
- [Scott and Miklowitz 1967] R. A. Scott and J. Miklowitz, “Transient elastic waves in anisotropic plates”, *J. Appl. Mech. (ASME)* **34**:1 (1967), 104–110.
- [Sneddon 1972] I. N. Sneddon, *The use of integral transforms*, McGraw-Hill, New York, 1972.
- [Willis 1971] J. R. Willis, “Fracture mechanics of interfacial cracks”, *J. Mech. Phys. Solids* **19**:6 (1971), 353–368.

Received 29 Mar 2015. Revised 12 Jul 2015. Accepted 17 Jul 2015.

LOUIS MILTON BROCK: louis.brock@uky.edu

Department of Mechanical Engineering, College of Engineering, University of Kentucky, 265 RGAN, Lexington, KY 40506-0503, United States

JOURNAL OF MECHANICS OF MATERIALS AND STRUCTURES

msp.org/jomms

Founded by Charles R. Steele and Marie-Louise Steele

EDITORIAL BOARD

ADAIR R. AGUIAR	University of São Paulo at São Carlos, Brazil
KATIA BERTOLDI	Harvard University, USA
DAVIDE BIGONI	University of Trento, Italy
YIBIN FU	Keele University, UK
IWONA JASIUK	University of Illinois at Urbana-Champaign, USA
C. W. LIM	City University of Hong Kong
THOMAS J. PENCE	Michigan State University, USA
DAVID STEIGMANN	University of California at Berkeley, USA

ADVISORY BOARD

J. P. CARTER	University of Sydney, Australia
D. H. HODGES	Georgia Institute of Technology, USA
J. HUTCHINSON	Harvard University, USA
D. PAMPLONA	Universidade Católica do Rio de Janeiro, Brazil
M. B. RUBIN	Technion, Haifa, Israel

PRODUCTION production@msp.org

SILVIO LEVY Scientific Editor

Cover photo: Mando Gomez, www.mandolux.com

See msp.org/jomms for submission guidelines.

JoMMS (ISSN 1559-3959) at Mathematical Sciences Publishers, 798 Evans Hall #6840, c/o University of California, Berkeley, CA 94720-3840, is published in 10 issues a year. The subscription price for 2015 is US\$565/year for the electronic version, and \$725/year (+\$60, if shipping outside the US) for print and electronic. Subscriptions, requests for back issues, and changes of address should be sent to MSP.

JoMMS peer-review and production is managed by EditFLOW[®] from Mathematical Sciences Publishers.

PUBLISHED BY

 **mathematical sciences publishers**
nonprofit scientific publishing

<http://msp.org/>

© 2015 Mathematical Sciences Publishers

- Relation between the Maxwell equations and boundary conditions in piezoelectric and piezomagnetic fracture mechanics and its application** HAO TIAN-HU **447**
- Axisymmetric loading of an elastic-plastic plate on a general two-parameter foundation**
 LUCA LANZONI, ANDREA NOBILI, ENRICO RADI and ANDREA SORZIA **459**
- Contours for planar cracks growing in three dimensions: Illustration for transversely isotropic solid** **LOUIS MILTON BROCK** **481**
- On Cesàro means of energy in micropolar thermoelastic diffusion theory**
 MARIN MARIN and SAMY REFAHY MAHMOUD **497**
- Topology optimization of spatial continuum structures made of nonhomogeneous material of cubic symmetry**
 RADOSŁAW CZUBACKI and TOMASZ LEWIŃSKI **519**